

A High-Pressure Polarized ^3He Gas Target for Nuclear Physics Experiments Using A Polarized Photon Beam

Q. Ye, G. Laskaris, W. Chen, H. Gao, W. Zheng, X. Zong

Triangle Universities Nuclear Laboratory and

Department of Physics, Duke University, Durham, NC 27708, USA

T. Averett

Department of Physics, College of William and Mary, Williamsburg, VA , USA

G. D. Cates, W. A. Tobias

Department of Physics, University of Virginia, Charlottesville, VA 22904, USA

Following the first experiment on three-body photodisintegration of polarized ^3He utilizing circularly polarized photons from High Intensity Gamma Source (HI γ S) at Duke Free Electron Laser Laboratory (DFELL), a new high-pressure polarized ^3He target cell made of pyrex glass coated with a thin layer of sol-gel doped with aluminum nitrate nonahydrate has been built in order to reduce photon beam induced backgrounds. The target is based on the technique of spin-exchange optical pumping of hybrid rubidium and potassium and the highest polarization achieved is $\sim 62\%$ determined from both NMR-AFP and EPR polarimetry. The X parameter is estimated to be 0.17 ± 0.06 and the performance of the target is in good agreement with theoretical predictions. We also present beam test results from this new target cell and the comparison with the GE180 ^3He target cell used previously at HI γ S. This is the first time that sol-gel coating technique has been used in a polarized ^3He target for nuclear physics experiments.

PACS numbers: 29.25.Pj, 67.30.ep, 76.60.-k, 34.50.Ez

I. INTRODUCTION

Quantum chromodynamics (QCD) is the theory of strong interaction in terms of quark and gluon degrees of freedom. While QCD has been well tested in the high energy regime where perturbative calculations can be carried out, it is still unsolved in the low energy, non-perturbative regime. Understanding the structure of the nucleon from the underlying theory of QCD, a fundamental and challenging task in nuclear and particle physics, remains an area of active research. With developments in polarized beam, recoil polarimetry, and polarized target technologies, polarization experiments have provided new observables on quantities related to the nucleon structure.

The High Intensity Gamma Source (HI γ S) at the Duke Free Electron Laser Laboratory (DFELL) opens a new window to studies of fundamental quantities related to the structure of the nucleon through polarized Compton scattering from polarized targets [1]. Such measurements allow access to nucleon spin polarizabilities, which describe the response of a spin-aligned nucleon to a quasi-static external electromagnetic field. Since there are no stable free neutron targets, effective neutron targets, such as deuteron and ^3He , are commonly used. A polarized ^3He target is an effective polarized neutron target [2, 3] due to the fact that the neutron is $\sim 90\%$ polarized in a polarized ^3He nucleus. There have been extensive studies employing polarized ^3He targets to extract the neutron electromagnetic form factors [4, 5, 6, 7, 8, 9], and neutron spin structure functions [10, 11, 12, 13, 14]. To extract

information on neutron using a polarized ^3He target, nuclear corrections need to be applied which rely on the state-of-the-art calculations of three-body systems.

The HI γ S facility also provides unique opportunities to test the three-body calculations. In 2008, a first measurement of double polarized three-body photodisintegration of ^3He was carried out at HI γ S [15] with an incident gamma beam energy of 11.4 MeV. In addition to providing tests of three-body calculations, three-body photodisintegration of ^3He is of further importance to experimental tests of the Gerasimov-Drell-Hearn (GDH) sum rule [16]. In this experiment, a high-pressure, longitudinally polarized ^3He gas target [17] and a circularly polarized photon beam were employed. Seven liquid scintillator detectors were placed around the ^3He target to detect the neutrons from the three-body breakup channel. The ^3He gas target cell was made of aluminosilicate (GE180) glass. This type of glass has fewer magnetic impurities and is less permeable to ^3He atoms than regular pyrex glass. However, the rich concentration of barium in the GE180 glass produced a large amount of background events in the neutron detectors. To reduce the background for future measurements at HI γ S, a new high-pressure ^3He cell made of sol-gel coated pyrex glass has been developed and tested.

The coating technique was developed by doping sol-gel with aluminum nitrate nonahydrate ($\text{Al}(\text{NO}_3)_3 \cdot 9\text{H}_2\text{O}$) [18, 19]. This method produces a glass with better homogeneity and higher purity via a chemical route. Single sealed pyrex cells produced using the sol-gel coating technique have yielded longer

relaxation times than those from cells without the coating [18]. This is the first time that this technique has been applied to a high-pressure ^3He target, a double-cell system for nuclear physics experiments. The smooth paramagnetic-free aluminosilicate glass coated surface reduces the probability of ^3He depolarization from the wall. Its low ^3He permeability helps prevent the loss of ^3He atoms. This allows long-term operation at temperatures typical of spin exchange optical pumping process (185°C for Rb-only-cells and 238°C for Rb-K hybrid cells). The target cell “BOLT” was coated at the University of Virginia and filled at the College of William and Mary. A photon beam test of BOLT at HI γ S was carried out in May, 2009. The rest of the paper is organized as the following. Section II describes the experimental apparatus and procedure. The target performance and a comparison between theoretical calculations and experimental results are presented in Section III. The in-beam test results of this new target are reported in Section IV.

II. EXPERIMENTAL APPARATUS AND PROCEDURE

A schematic of the experimental apparatus is shown in Fig. 1. It consists of a pair of Helmholtz coils with a

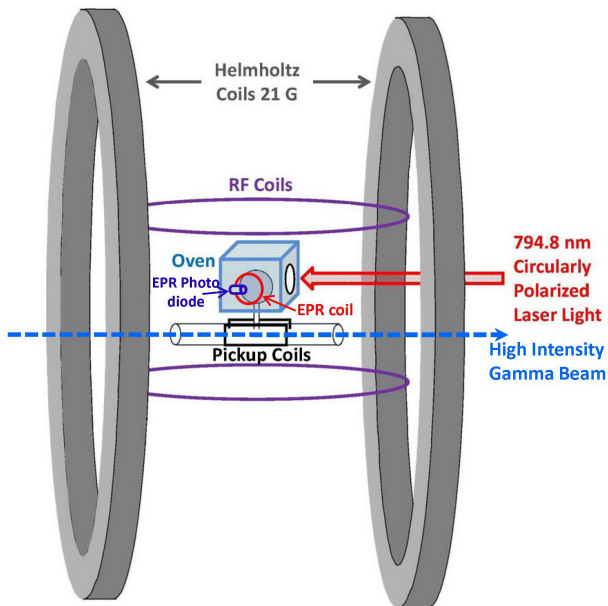


FIG. 1: (Color online) A schematic of the experimental setup.

diameter of 173 cm to provide a magnetic holding field with a typical value of 21 G. BOLT is a pyrex glass cell coated with aluminosilicate and contains a mixture of Rb-K. It consists of a spherical pumping chamber with a radius of 4.3 cm and a target chamber with a length

and a diameter of 38.7 cm and 3.1 cm, respectively. The chambers are connected by a tube that is 9 cm long with a diameter of 1.3 cm. The cell is installed in the center of the Helmholtz coils with the pumping chamber in the oven.

The ^3He polarization is measured using both the NMR-adiabatic fast passage (AFP) method [20] and the electron paramagnetic resonance (EPR) technique [21]. The AFP system includes two ~ 79 cm-diameter RF coils with a separation of 39.5 cm placed horizontally above and below the cell and a pair of rectangular pickup coils located on both sides of the target chamber, and perpendicular to both the holding field and the RF field. The EPR system includes an 7.6 cm diameter EPR coil inside the oven close to the pumping chamber and a photo diode to monitor the EPR signal. Details of the polarimetry systems can be found in [17]. The ^3He nuclei are polarized through spin-exchange optical pumping. Three lasers with three separate sets of optics are used to produce circularly polarized laser light. After the optics, the net output power of the two Coherent DUO-FAP broadband lasers is ~ 78 W and the third Spectra-Physics narrowed laser has a net power output of 23 W.

Before the ^3He nuclei are polarized, the cell is heated to 120°C in a separate oven and a tunable laser is used to probe the line shape of the Rb D_1 transition. Collisions between Rb and ^3He can broaden the resonance lines of rubidium so that the width is proportional to the density of ^3He in the cell [22]. By measuring the width of the D_1 line, the density of ^3He is determined to be 5.16 ± 0.29 amagats. To polarize the ^3He nuclei, the pumping chamber is heated up in the oven by air flowing through three heaters. The pressure inside the cell is ~ 7.66 atms with the pumping chamber at 238°C and target chamber at 60°C . The Rb atoms in the pumping chamber are polarized through the optical pumping process and then transfer angular momentum to the K atoms. The spin exchange collisions between K and ^3He and between Rb and ^3He subsequently polarize the ^3He nuclei [23]. The time to reach the maximum polarization for such a Rb-K hybrid cell is much faster than a Rb-only cell due to the higher efficiency for spin exchange polarization of ^3He by K [24].

The ^3He polarization measured by the NMR-AFP method is recorded every three hours during the polarization accumulation period (“pump-up” period). After the polarization has reached a maximum, EPR measurements are carried out to measure the absolute ^3He polarization, which can be compared to the value from the NMR signal after water calibration [20]. With the lasers off and the alkali no longer in vapor form, AFP measurements are continued in order to measure the spin-lattice relaxation time, T_1 , in the cell.

The systematic error of the relaxation time is dominated by the uncertainty in the determination of the AFP losses, which is derived by fitting n consecutive AFP

measurements to $A_0(1-L)^n$, where L is the AFP inefficiency parameter. The relaxation times are obtained from the exponential decay of the AFP signal strength as a function of time, corrected for the AFP losses. The AFP system uses an RF amplifier to power the RF coils for the spin flip during the measurement, but the RF amplifier is left off during the time intervals between AFP measurements to prevent the polarized ^3He atoms from depolarizing due to the wide band amplified RF noise. The AFP signals during the pump-up period are fitted to $A_0(1-e^{-t/T_p})$, where T_p is the effective pump-up time for the double-cell system.

III. RESULTS AND DISCUSSION

The three major contributions to ^3He depolarization are the ^3He dipole-dipole relaxation mechanism, the magnetic field gradient effect and the surface effect on the cell wall. The dipole-dipole relaxation time is calculated to be ~ 142 hours for BOLT [25]. The relaxation time due to the magnetic field gradient in our system is calculated to be over 500 hours [26] from the magnetic field mapping data. The measured pump-up times, T_p , maximum NMR and EPR signals, and the double-cell room temperature relaxation times, T_1 , are listed in Table I. Since the measured values for T_1 are much shorter than the relaxation times from the dipole-dipole effect and the gradient effect, the wall effect on the cell's surface is the most significant contribution to the relaxation of polarized ^3He .

TABLE I: Pump-up time (T_p), maximum NMR signal, maximum EPR signal, relaxation time (T_1) from different measurements, statistical uncertainties included.

Run no.	T_p (hr)	NMR(mV)	EPR(kHz)	T_1 (hr)
1	9.34±0.27	17.31±0.01	39.12±0.32	34.40±0.31
2	8.38±0.17	17.71±0.01	38.57±0.27	33.59±0.12
3	8.80±0.21	17.47±0.01	40.95±0.27	33.0±0.04

The weighted maximum NMR signal and EPR frequency are (17.50±0.01) mV and (39.59±0.16) kHz, respectively. After comparing with the water NMR signal [20], the absolute ^3He polarization in the target chamber is determined to be (60.9±4.1)%. Since the EPR constant [21] for our cell is 1.57±0.09, the measured EPR frequency shift corresponds to a ^3He polarization of (62.1±3.6)%, which is consistent with the result from the NMR-AFP after the water calibration. The uncertainty is dominated by the uncertainty in the ^3He number density of the cell.

In order to calculate the theoretically achievable maximum polarization of ^3He in BOLT, the alkali metal's polarization is estimated first. The Rb's polarization at

any given location along the laser beam is [27]

$$P_{Rb}(z, P) = \frac{R(z, P)}{R(z, P) + \Gamma'_{Rb}} \quad (1)$$

where $R(z, P) = \int \phi(z, \nu, P) \sigma_{Rb}(\nu) d\nu$ is the optical pumping rate at a certain location and Γ'_{Rb} is the total spin destruction rate. $\phi(z, \nu, P)$ is the number of photons per unit area A per unit time in the frequency interval $d\nu$ ($d\nu = \frac{c}{\lambda^2} \delta\lambda$) along the laser beam direction \hat{z} with a given z and ν . In our case, $A=48.3$ cm² and the FWHM of the broad band diode-laser is $\delta\lambda=4$ nm. $\sigma_{Rb}(\nu) = \frac{\sigma_{Rb0}}{1+4\Delta^2/\gamma_{Rb}^2}$ [27] is the frequency interval absorption cross section, assuming a Lorentzian form, where the peak cross section is $\sigma_{Rb0} = 3.2 \times 10^{-13}$ cm². $\Delta = \nu - \nu_0$ is the frequency offset from the optical pumping resonant frequency ν_0 ($\lambda_0=794.8$ nm), and $\gamma_{Rb} = (18.7 \pm 0.3)$ GHz/amg [22] is the pressure broadened width of the D₁ transition of Rb. $\phi(z, \nu, P)$ can be expressed with respect to the power P and the frequency of the laser as well as the location along the laser beam [21, 27] (see Appendix I).

$$\phi(z, \nu, P) \cong \frac{P}{Ah\nu_0 d\nu} e^{-[Rb]\sigma_{Rb}(\nu)(1-P_\infty P_{Rb}(z, P))z} \quad (2)$$

where $[Rb]$ is the Rb number density and P_∞ is the mean photon spin of the pumping light. It follows that the pumping rate at a certain location z is given by (see Appendix I)

$$R(z, P) \cong \varepsilon \frac{\pi \sigma_{Rb0} \gamma_{Rb} P}{2Ah\nu_0 d\nu} e^{-[Rb]\sigma_{Rb0}(1-P_\infty P_{Rb}(z, P))z/2} \cdot J_0\left(-[Rb]\sigma_{Rb0}(1-P_\infty P_{Rb}(z, P))z/2\right) \quad (3)$$

where J_0 is the zeroth order Bessel function of the first kind and $\varepsilon \sim 0.75$ is an experimental parameter of the laser power loss due to the oven window and the cell's glass wall. The equation suggests that Rb atoms are polarized to different degrees throughout the cell volume. However, since Rb atoms are moving fast at a thermal velocity of $\sim 10^2$ m/s in the pumping chamber, they are polarized uniformly and will reach the same polarization as the atoms at $z = 0$, which is $P_{Rb}(z = 0, P) = \frac{R(z=0, P)}{R(z=0, P) + \Gamma'_{Rb}}$, where $R(z = 0, P) \sim (6.0 \times 10^2 P)$ Hz. The total spin destruction rate $\Gamma'_{Rb} = \Gamma_{Rb} + D_r \Gamma_K + q_{KR}[K]$ [27] is calculated to be ~ 1 kHz where the alkali vapor density ratio is $D_r = \frac{[K]}{[Rb]} = 0.96$, the nitrogen pressure $P_{N_2} = 75$ torr at room temperature, the pumping chamber temperature 511 K, and the target chamber temperature 338 K. $q_{KR} = 2.2 \times 10^{-13}$ cm³/s is the geometric mean between the Rb-Rb and K-K spin destruction rates. With the measured laser power of 78 W after all the optics from the two broadband Coherent diode lasers, the Rb polarization is calculated to be $P_{Rb} = (97.9 \pm 0.1)\%$. The additional 23 W narrowed

band laser has a FWHM of $\delta\lambda = 0.4$ nm and corresponds to 230 W of broad band laser in the ideal case. The polarization of Rb can then reach $\sim 99.5\%$. However in reality, the contribution from the narrowed laser is limited due to the off-resonance laser wavelength.

After the Rb polarization is calculated, the polarization of ^3He can be estimated by employing equation (A43) in [28]. This equation needs to be modified according to equation (2) in [29] (or (1) in [30]) in order to include the X parameter which is a phenomenological parameter that reflects additional unknown spin decay processes. The ^3He polarization in both the pumping and target chambers is then given by (see Appendix II)

$$P_{3\text{He}} = P_{\text{Rb}}(z=0, P) \frac{f_{\text{opc}} \cdot \gamma_{\text{se}}^{\text{Rb/K}}}{f_{\text{opc}} \cdot \gamma_{\text{se}}^{\text{Rb/K}} (1 + X) + 1/T_1} \quad (4)$$

where $\gamma_{\text{se}}^{\text{Rb/K}}$ is the spin exchange rate of Rb and K with ^3He and $f_{\text{opc}} = 0.38$ is the fraction of atoms in the pumping chamber. Since $T_p = \frac{1}{\Gamma_{3\text{He}}}$ and $\Gamma_{3\text{He}} = f_{\text{opc}} \cdot \gamma_{\text{se}}^{\text{Rb/K}} (1 + X) + 1/T_1$ [30], we have

$$\gamma_{\text{se}}^{\text{Rb/K}} = \frac{P_{3\text{He}}}{f_{\text{opc}} \cdot P_{\text{Rb}} \cdot T_p} \quad (5)$$

$$\frac{1}{T_p} = f_{\text{opc}} \cdot \gamma_{\text{se}}^{\text{Rb/K}} (1 + X) + 1/T_1 \quad (6)$$

The weighted experimental pump-up time and relaxation time of BOLT at room temperature are $T_p = (8.70 \pm 0.12)$ hrs and $T_1 = (33.08 \pm 0.04)$ hrs, respectively. Using the experimental value of the ^3He polarization, the X parameter can be estimated using equation (5) and (6) to be 0.17 ± 0.06 . The theoretical spin exchange rate is given by $\gamma_{\text{se}}^{\text{Rb/K}} = k_{\text{se}}^{\text{Rb}}[\text{Rb}] + k_{\text{se}}^{\text{K}}[\text{K}] = 7.4 \times 10^{-5}$ Hz [27, 30], where $k_{\text{se}}^{\text{Rb}} = 6.8 \times 10^{-20}$ cm³/s [24, 33] and $k_{\text{se}}^{\text{K}} = 5.5 \times 10^{-20}$ cm³/s [34]. The ^3He polarization can then be calculated and plotted versus the input laser power by inserting equation (1) into equation (4) along with the X parameter and the theoretical spin exchange rate. The ^3He polarization reaches a value of $P_{3\text{He}} = (66.5 \pm 2.5)\%$ with an input broad band laser power of 78 W. In the ideal case with 308 W input broad band laser power, the ^3He polarization can reach $\sim 67.6\%$. The experimental value is in good agreement with this theoretical calculation.

IV. BEAM TEST

An in-beam test of BOLT was carried out at HI γ S in May, 2009. Three liquid organic scintillator detectors [31] filled with BC-501A fluid from the Bicorn Corporation were placed at 50° , 90° , 130° and 90 cm, 75 cm, 90 cm away from the center of the target, respectively. A vertical multi-layer motor-controlled support was used to place different targets in the gamma beam. The targets included N₂ gas targets in both pyrex and GE180 glass

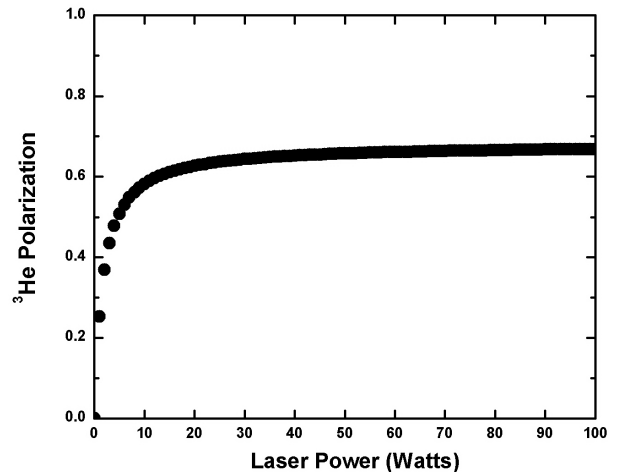


FIG. 2: The theoretical ^3He polarization versus the input broad band laser power.

cells, BOLT, and a GE180 glass cell “Linda”. A thin aluminum plate, liquid D₂O target and D₂ gas targets were available for detector calibration purposes. All N₂ and ^3He target cells have the same dimensions.

The energy of the photon beam was 11.4 MeV and the photon flux was $\sim 1.5 \times 10^7$ /s monitored by a three-paddle system [32] right after the photon beam’s collimator and a 4.7 cm thick liquid D₂O target placed downstream of the ^3He target with two neutron detectors at 90° on both sides. Compared to the position in the experiment [15], the ^3He target was pushed ~ 2 meters downstream due to another experimental apparatus in the beamline.

Fig. 3 shows the results of the in-beam test. The points represent the neutron events’ ratios between two N₂ cells made of pyrex glass and GE180 glass and two ^3He cells made of pyrex (BOLT) and GE180 (Linda) glass. All the neutron events were selected from the raw data after the multiplicity cut, pulse shape discrimination cut, pulse height cut and time of flight cut [32] and had energies ranging from 1 MeV to 2.5 MeV. The numbers are also shown in Table II.

TABLE II: Results of the in-beam test. The ratios between the number of events from N₂ and ^3He cells made from pyrex and GE180 glass are listed.

Detector	Ratio between N ₂ cells	Ratio between ^3He cells
50°	$85.3 \pm 6.0\%$	$93.5 \pm 5.7\%$
90°	$67.6 \pm 5.9\%$	$75.2 \pm 5.0\%$
130°	$65.5 \pm 6.7\%$	$70.3 \pm 6.0\%$

Since the ^3He target was placed farther downstream in this experiment, the liquid D₂O target and the longer air path generated considerably more background neutrons.

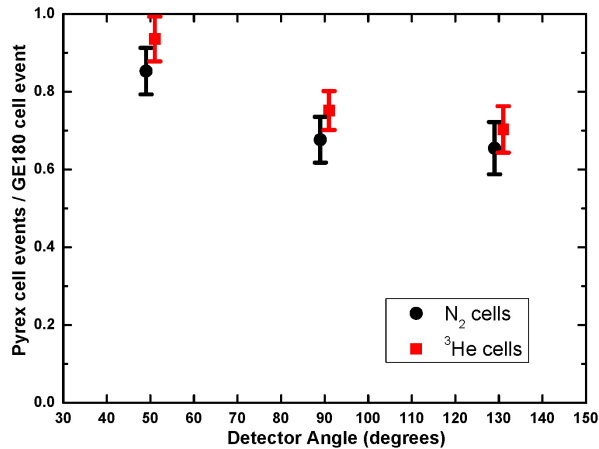


FIG. 3: (Color online) Results of the in-beam test. Black circles represent the ratios between the events from pyrex glass N₂ cell and GE180 glass N₂ cell at three detectors together with the statistical uncertainties. The red squares represent the ratios between the events from BOLT and Linda at three detectors together with the statistical uncertainties.

In the 50° detectors, the yield difference is smaller since they are closer to the liquid D₂O target and the background contamination dilutes the difference. The improvement using BOLT for future experiments compared with Linda should be better than the results presented in Fig. 3 for an optimal target position, where the background neutron events can be minimized. Furthermore, plans have been made to employ more stable, higher flux (at least $5 \times 10^7/s$) photon beams, better shielding from the downstream D₂O target and a vacuum pipe between the beam source and the target. All these measures will help reduce the neutron background further for better statistics.

V. SUMMARY

We have tested the world's first high-pressure hybrid ³He pyrex glass cell coated with a thin aluminosilicate glass and have achieved a polarization of $\sim 62\%$ determined by both NMR-AFP and EPR methods. This value compares favorably with the predicted maximum theoretical ³He polarization value. The X parameter is measured for the first time in a double-cell system to be 0.17 ± 0.06 . The in-beam test shows that the sol-gel coated pyrex glass target generates fewer neutron background events than the GE180 glass cell. This new type of target will be important for the future Compton scattering and GDH experiments at HI γ S.

VI. ACKNOWLEDGMENT

The authors wish to thank Michael Souza of Princeton University for making the target cell reported in this work, Alexandre Deur for providing us with chemical information for the GE180 glass, K. Kluttz for helpful comments about this work, Yi Qiang and Yi Zhang for their help with the target density measurement, N. Brown, M. Emamian, S. Henshaw, B. Perdue and H. Weller for helping with the target alignment, M. Pentico, V. Rathbone, C. Sun and Y. Wu for the gamma beam operation, B. Carlin and C. Westerfeld for the technical support. This work is supported by the U.S. Department of Energy under contract number DE-FG02-03ER41231 and Duke University.

APPENDIX I

The calculation of $\phi(z, \nu, P)$ (equation (2)) assumes that the spectrum of the laser has a Gaussian form and the power P is concentrated in the FWHM $\delta\lambda$. This is an approximation because some of the laser power lies in the tails of the Gaussian.

In order to find the optical pumping rate $R(z, P)$ (equation (3)), a second approximation is needed. Since

$$\begin{aligned} R(z, P) &= \int_0^\infty \phi(z, \nu, P) \sigma_{Rb}(\nu) d\nu \\ &= \frac{P}{Ah\nu_0 d\nu} \int_0^\infty e^{-\xi \sigma_{Rb}(\nu)} \sigma_{Rb}(\nu) d\nu \end{aligned} \quad (7)$$

where $\xi = [Rb](1 - P_\infty P_{Rb}(z, P))z$. If the substitution $x = \frac{2\Delta}{\gamma_{Rb}}$ is made, the equation becomes

$$R(z, P) = \frac{\sigma_{Rb0} \gamma_{Rb} P}{2Ah\nu_0 d\nu} \int_{-\frac{2\nu_0}{\gamma_{Rb}}}^\infty e^{-\frac{\xi}{1+x^2}} \frac{1}{1+x^2} dx \quad (8)$$

This integral is approximately equal to

$$R(z, P) \cong \frac{\sigma_{Rb0} \gamma_{Rb} P}{2Ah\nu_0 d\nu} \int_{-\infty}^\infty e^{-\frac{\xi}{1+x^2}} \frac{1}{1+x^2} dx \quad (9)$$

for any numerical value of ξ . Since the integration function is symmetric w.r.t. 0, equation (9) equals

$$R(z, P) \cong \frac{\sigma_{Rb0} \gamma_{Rb} P}{Ah\nu_0 d\nu} \int_0^\infty e^{-\frac{\xi}{1+x^2}} \frac{1}{1+x^2} dx \quad (10)$$

After a change of variable $y = \frac{1}{1+x^2}$ is made

$$R(z, P) \cong \frac{\sigma_{Rb0} \gamma_{Rb} P}{2Ah\nu_0 d\nu} \int_0^1 \frac{1}{\sqrt{(1-y)y}} e^{-\xi y} dy \quad (11)$$

Solving it gives equation (3).

APPENDIX II

The rate equations for a double-cell system are given by (rate equations in [28] with the X parameter included)

$$\frac{dP_p}{dt} = -G_p(P_p - P_t) - ((1 + X)f_{opc}\gamma_{se}^{Rb/K} + \Gamma_p)P_p + P_{Rb}f_{opc}\gamma_{se}^{Rb/K} \quad (12)$$

$$\frac{dP_t}{dt} = G_t(P_p - P_t) - \Gamma_t P_t \quad (13)$$

$$P_p(0) = P_t(0) = 0; P_p'(\infty) = P_t'(\infty) = 0 \quad (14)$$

The assumptions are that the alkali metals are confined in the pumping chamber only and the sources of ^3He polarization in the pumping chamber are spin exchange between alkali metals and ^3He and diffusion of polarized ^3He atoms from the target cell. Relaxation in the pumping (target) chamber is due to the combined relaxation mechanisms (dipole-dipole effect, magnetic field gradient effect and wall effect) and ^3He diffusion to the target (pumping) chamber. The G_p is the polarized ^3He transfer rate from the pumping cell to the target cell and G_t is the transfer rate in the other direction (Appendix in [28]). They are defined as

$$G_p = \frac{D_p S}{L V_p} \quad (15)$$

$$G_t = \frac{D_t S}{L V_t} \quad (16)$$

where S , L are the cross-sectional area and length of the connecting tube between the pumping chamber and

target chamber. $D_{p(t)}$ and $V_{p(t)}$ are the ^3He diffusion coefficient and volume of each chamber, respectively. The diffusion coefficient is given by $D = \frac{\bar{v}\lambda}{3}$ where \bar{v} is the ^3He mean thermal velocity and λ is the mean free path. The total theoretical transfer rate is equal to $G = G_p + G_t$.

The relaxation rates are defined as (equation (6) in [28])

$$\Gamma_p = \Gamma'_p \frac{n_p V_p}{n_p V_p + n_t V_t} \quad (17)$$

$$\Gamma_t = \Gamma'_t \frac{n_t V_t}{n_p V_p + n_t V_t} \quad (18)$$

where Γ'_p and Γ'_t are the averaged relaxation rates in the pumping and target chambers. Theoretically, the spin exchange rate is given by $\gamma_{se}^{Rb/K} = k_{se}^{Rb}[Rb] + k_{se}^K[K]$ [30].

The general time-dependent solution of this coupled equations system is given by

$$\begin{aligned} P_p(t) = & \frac{(G_t + \Gamma_t)P_{Rb}f_{opc}\gamma_{se}^{Rb/K}}{(G_p + f_{opc}\gamma_{se}^{Rb/K}(1 + X) + \Gamma_p)(G_t + \Gamma_t) - G_p G_t} + \frac{P_{Rb}f_{opc}\gamma_{se}^{Rb/K}}{\sqrt{(G_p + f_{opc}\gamma_{se}^{Rb/K}(1 + X) + \Gamma_p - G_t - \Gamma_t)^2 + 4G_p G_t}} \\ & \cdot \left[-\frac{G_p + f_{opc}\gamma_{se}^{Rb/K}(1 + X) + \Gamma_p - G_t - \Gamma_t + \sqrt{(G_p + f_{opc}\gamma_{se}^{Rb/K}(1 + X) + \Gamma_p - G_t - \Gamma_t)^2 + 4G_p G_t}}{G_p + f_{opc}\gamma_{se}^{Rb/K}(1 + X) + \Gamma_p + G_t + \Gamma_t + \sqrt{(G_p + f_{opc}\gamma_{se}^{Rb/K}(1 + X) + \Gamma_p - G_t - \Gamma_t)^2 + 4G_p G_t}} \right. \\ & \cdot e^{-\frac{1}{2}(G_p + f_{opc}\gamma_{se}^{Rb/K}(1 + X) + \Gamma_p + G_t + \Gamma_t + \sqrt{(G_p + f_{opc}\gamma_{se}^{Rb/K}(1 + X) + \Gamma_p - G_t - \Gamma_t)^2 + 4G_p G_t})t} \\ & + \frac{G_p + f_{opc}\gamma_{se}^{Rb/K}(1 + X) + \Gamma_p - G_t - \Gamma_t - \sqrt{(G_p + f_{opc}\gamma_{se}^{Rb/K}(1 + X) + \Gamma_p - G_t - \Gamma_t)^2 + 4G_p G_t}}{G_p + f_{opc}\gamma_{se}^{Rb/K}(1 + X) + \Gamma_p + G_t + \Gamma_t - \sqrt{(G_p + f_{opc}\gamma_{se}^{Rb/K}(1 + X) + \Gamma_p - G_t - \Gamma_t)^2 + 4G_p G_t}} \\ & \cdot e^{-\frac{1}{2}(G_p + f_{opc}\gamma_{se}^{Rb/K}(1 + X) + \Gamma_p + G_t + \Gamma_t - \sqrt{(G_p + f_{opc}\gamma_{se}^{Rb/K}(1 + X) + \Gamma_p - G_t - \Gamma_t)^2 + 4G_p G_t})t} \left. \right] \quad (19) \end{aligned}$$

$$\begin{aligned}
P_t(t) = & \frac{G_t P_{Rb} f_{opc} \gamma_{se}^{Rb/K}}{(G_p + f_{opc} \gamma_{se}^{Rb/K} (1+X) + \Gamma_p)(G_t + \Gamma_t) - G_p G_t} + \frac{2G_t P_{Rb} f_{opc} \gamma_{se}^{Rb/K}}{\sqrt{(G_p + f_{opc} \gamma_{se}^{Rb/K} (1+X) + \Gamma_p - G_t - \Gamma_t)^2 + 4G_p G_t}} \\
& \cdot \left[\frac{1}{G_p + f_{opc} \gamma_{se}^{Rb/K} (1+X) + \Gamma_p + G_t + \Gamma_t + \sqrt{(G_p + f_{opc} \gamma_{se}^{Rb/K} (1+X) + \Gamma_p - G_t - \Gamma_t)^2 + 4G_p G_t}} \right. \\
& \cdot e^{-\frac{1}{2}(G_p + f_{opc} \gamma_{se}^{Rb/K} (1+X) + \Gamma_p + G_t + \Gamma_t + \sqrt{(G_p + f_{opc} \gamma_{se}^{Rb/K} (1+X) + \Gamma_p - G_t - \Gamma_t)^2 + 4G_p G_t})t} \\
& - \frac{1}{G_p + f_{opc} \gamma_{se}^{Rb/K} (1+X) + \Gamma_p + G_t + \Gamma_t - \sqrt{(G_p + f_{opc} \gamma_{se}^{Rb/K} (1+X) + \Gamma_p - G_t - \Gamma_t)^2 + 4G_p G_t}} \\
& \left. \cdot e^{-\frac{1}{2}(G_p + f_{opc} \gamma_{se}^{Rb/K} (1+X) + \Gamma_p + G_t + \Gamma_t - \sqrt{(G_p + f_{opc} \gamma_{se}^{Rb/K} (1+X) + \Gamma_p - G_t - \Gamma_t)^2 + 4G_p G_t})t} \right] \quad (20)
\end{aligned}$$

Using condition $P'_p(\infty) = P'_t(\infty) = 0$, the equilibrium ^3He polarization in each chamber is

$$P_p(t \rightarrow \infty) = \frac{(G_t + \Gamma_t) P_{Rb} f_{opc} \gamma_{se}^{Rb/K}}{(G_p + f_{opc} \gamma_{se}^{Rb/K} (1+X) + \Gamma_p)(G_t + \Gamma_t) - G_p G_t} \quad (21)$$

$$P_t(t \rightarrow \infty) = \frac{G_t \cdot P_{Rb} f_{opc} \gamma_{se}^{Rb/K}}{(G_p + f_{opc} \gamma_{se}^{Rb/K} (1+X) + \Gamma_p)(G_t + \Gamma_t) - G_p G_t} \quad (22)$$

The transfer rate is also measured experimentally by destroying the polarization in the target chamber using a rectangular RF coil, and measuring the recovery of the NMR free induction decay signal as polarized ^3He atoms

diffuse into the target chamber from the pumping chamber. The rate is measured to be $\sim \frac{1}{50 \text{ mins}}$, which is much bigger than the spin relaxation rate $\sim \frac{1}{33 \text{ hrs}}$. So it is assumed that $G_t + \Gamma_t \simeq G_t$. And we have

$$P_p(t \rightarrow \infty) = P_t(t \rightarrow \infty) = \frac{G_t P_{Rb} f_{opc} \gamma_{se}^{Rb/K}}{(G_p + f_{opc} \gamma_{se}^{Rb/K} (1+X) + \Gamma_p)(G_t + \Gamma_t) - G_p G_t} \quad (23)$$

Assuming that $G_p \simeq G_t$, the equation becomes

$$P_{^3\text{He}} = P_{Rb}(z=0, P) \frac{f_{opc} \gamma_{se}^{Rb/K}}{f_{opc} \gamma_{se}^{Rb/K} (1+X) + 1/T_1} \quad (24)$$

where $\Gamma = \frac{1}{T_1} = \Gamma_p + \Gamma_t$ is the total relaxation rate.

- [2] J. L. Friar, B. F. Gibson, G. L. Payne, A. M. Bernstein, and T. E. Chupp, Phys. Rev. C **42**, 2310, 1990.
- [3] B. Blankleider and R. M. Woloshyn, Phys. Rev. C, **29**, 538, 1984.
- [4] H. Gao *et al.*, Phys. Rev. C, **50**, R546, 1994.
- [5] M. Meyerhoff *et al.*, Phys. Lett. B, **327**, 201, 1994.
- [6] J. Becker *et al.*, Eur. Phys. J. A, **6**, 329, 1999.
- [7] D. Rohe *et al.*, Phys. Rev. Lett. **83**, 4257, 1999.
- [8] W. Xu *et al.*, Phys. Rev. Lett., **85**, 2900, 2000; Phys. Rev. C, **67**, 012201, 2003; B. Anderson *et al.* (E95-001 Collaboration), Phys. Rev. C, **75**, 034003, 2007.
- [9] J. Bermuth *et al.*, Phys. Lett. B, **564**, 199, 2003.
- [10] P. L. Anthony *et al.*, Phys. Rev. D, **54**, 6620, 1996.
- [11] K. Abe *et al.*, Phys. Rev. Lett., **79**, 26, 1997.

[1] H. R. Weller, M. Ahmed, H. Gao, Tornow *et al.*, *Progress in Particle and Nuclear Physics*, DOI: 10.1016/j.pnpnp.2008.07.001.

- [12] K. Ackerstaff *et al.*, Phys. Lett. B, **404**, 383, 1997.
- [13] X. Zheng *et al.*, Phys. Rev. Lett., **92**, 012004, 2004.
- [14] M. Amarian *et al.*, Phys. Rev. Lett., **89**, 242301-1, 2002; Phys. Rev. Lett., **92**, 022301, 2004.
- [15] X. Zong *et al.*, to be submitted.
- [16] S. D. Drell *et al.*, Phys. Rev. Lett., **16**, 908, 1966; S. B. Gerasimov, Sov. J. Nucl. Phys., **2**, 430, 1966.
- [17] K. Kramer, X. Zong, R. Lu, D. Dutta, H. Gao, X. Qian, Q. Ye, X. Zhu, T. Averett, S. Fuchs, Nuclear Instruments and Methods in Physics Research A, **582**, 318, 2007.
- [18] M.F. Hsu *et al.*, Applied Phys. Lett. **77**, number 13, 2069 (2000).
- [19] W. A. Tobias, G. D. Cates, J. Chaput, A. Deur, S. Rohrbaugh, and J. Singh, "Application of Sol-Gel technology to high pressure polarized ^3He nuclear targets", Department of Physics, University of Virginia.
- [20] W. Lorenzon, T. R. Gentile, H. Gao, R. D. McKeown, Phys. Rev. A, **47**, 468, 1993.
- [21] M. V. Romalis and G. D. Cates, Phys. Rev. A, **58**, 3004, 1998.
- [22] M. V. Romalis, E. Miron, and G. D. Cates, Phys. Rev. A, **56**, 4569, 1997.
- [23] W. Happer, G. D. Cates, M. V. Romalis, C. J. Erickson, U. S. Patent No. 6318092 2001.
- [24] A. B. Baranga, S. Appelt, C. J. Erickson, A. R. Young, and W. Happer, Phys. Rev. A, **58**, 2282, 1998; A. B. Baranga, S. Appelt, M. V. Romalis, C. J. Erickson, A. R. Young, G. D. Cates and W. Happer, Phys. Rev. Lett., **80**, 2801, 1998.
- [25] N. R. Newbury, A. S. Barton, G. D. Gates, W. Happer, H. Middleton, Phys. Rev. A, **48**, 6, 1993.
- [26] G. D. Cates, S. R. Schaefer, and W. Happer, Phys. Rev. A, **37**, 2877, 1988.
- [27] W. C. Chen, T. R. Gentile, T. G. Walker and E. Babcock, Phys. Rev. A, **75**, 013416, 2007.
- [28] T. E. Chupp, R. A. Loveman, A. K. Thompson, A. M. Bernstein, and D. R. Tieger, Phys. Rev. C, **45**, 915, 1992.
- [29] B. Chann *et al.*, J. Appl. Phys., **94**, 6908, 2003.
- [30] E. Babcock, B. Chann, T. G. Walker, W. C. Chen, T. R. Gentile, Phys. Rev. Lett., **96**, 083003, 2006.
- [31] Alexander S. Crowell, Ph.D. thesis, Duke University, 2001.
- [32] Matthew Blackston, Ph.D. thesis, Duke University, 2007.
- [33] B. Chann, E. Babcock, L. W. Anderson, T. G. Walker, Phys. Rev. A, **66**, 032703, 2002.
- [34] E. Babcock, Ph. D. thesis, University of Wisconsin, Madison, 2005.